

Electrode Kinetics of Eu(III) Ion in the Presence of 1,4-Benzenedimethanol

Osamu IKEDA,* Katsuhiko TSUURA, and Hideo TAMURA

Department of Applied Chemistry, Faculty of Engineering, Osaka University, Yamada-ka, Suita, Osaka 565

(Received July 23, 1980)

In order to know the role of aromatic ring on the electrode kinetics, d. c. polarogram of Eu(III) ion was measured in the presence of 1,4-benzenedimethanol (1,4-BDM). The effect of the adsorption has been discussed by correlating the kinetic data to the adsorption behaviors of 1,4-BDM estimated from the electrocapillary curves. At the standard potential of Eu(III)/Eu(II) (-0.600 V *vs.* SCE), 1,4-BDM on the electrode changed its orientation from horizontal to vertical with an increase in the coverage. Both orientations showed an inhibition effect for the electroreduction of Eu(III) ion. When the coverage due to the horizontal orientation is less than 0.8, the inhibition was interpreted by an additional energy to deform the surface layer. On the other hand, the inhibition at full coverage due to both the horizontal and the vertical orientations was interpreted by the tunneling probability through the adsorbed layer differed in the thickness.

Electroinactive organic compounds adsorbed on the electrode influence the reduction rate of metal cations. It has been proposed that various factors influence the reduction rate, for example blocking effect,^{1–6)} interaction between the activated complex and the adsorbed ions or molecules,⁷⁾ additional energy to bring the discharging ion to the pre-electrode state,⁸⁾ electrostatic potential⁹⁾ and dipole,¹⁰⁾ and so on. The above factors have been reviewed by Lipkowski and Galus,¹¹⁾ and Damaskin and Afanas'ev.¹²⁾

Organic compounds adsorbed on the electrode usually inhibit the reduction rate of metal cations. However, Loshkarev *et al.*¹³⁾ observed that 1-naphthol inhibited the reduction rate of Bi(III) when its aromatic ring was vertical to the electrode surface, but it did not prevent the electron transfer to the discharging ion when the ring was horizontal. They explained these results on the basis of the idea proposed by Dyatkina and Damaskin¹⁴⁾ that aromatic compounds, adsorbed horizontally on the electrode, extend the metal surface toward the solution. Dutkiewicz and Paucz¹⁵⁾ have also discussed the electrode reaction of Cd(II) ion in the presence of benzenesulfonate ion on the same explanation as Loshkarev *et al.*¹³⁾ However, such an effect of aromatic compounds is observed only for the electroreduction of deposition type such as Bi(III)/Bi(0) and Cd(II)/Cd(0). It is of interest to study their effect on the electroreduction of simple charge transfer type, namely Eu(III)/Eu(II).

In this study, 1,4-benzenedimethanol (1,4-BDM) was chosen as the aromatic compound, because it has a good solubility in water and it is a neutral compound which does not form a complex with Eu(III) ion. The initial study was the adsorption behaviors of 1,4-BDM at the mercury/water interface, and then the effect of the adsorption on the electrode kinetics of Eu(III)/Eu(II).

Experimental

All chemicals were analytical grade materials. 1,4-Benzenedimethanol (1,4-BDM) was recrystallized twice from distilled water. Aqueous 1 M NaClO₄[†] prepared from triply distilled water was used as the supporting electrolyte, and was treated with purified active charcoal before use. Mer-

cury was purified by treatment with dilute nitric acid, then distilled triply in a vacuum. Nitrogen gas, after passing through a purification line, was used for deaeration.

Adsorption behaviors of 1,4-BDM were estimated from the analysis of the electrocapillary curves, which were measured with the maximum bubble pressure method.^{16,17)} Twelve different concentrations of 1,4-BDM solutions were prepared to cover between 0.2 mA and 15 mA. The interfacial tension was measured at 50 mV intervals, except for positive and negative extremes where 25 mV intervals were chosen. The error of the measurement was ± 0.1 mN m⁻¹ near the electrocapillary maximum, and ± 0.3 mN m⁻¹ at positive and negative extremes. Most of the parameters essential to adsorption were derived by analyzing the electrocapillary curves with a computer programme. At the analysis, no corrections were taken into consideration for the medium effect on the activity coefficient of the supporting electrolyte,^{18,19)} and the activity coefficient of the adsorbate.²⁰⁾

Differential capacity was measured with a cell and a bridge similar to those described by Hills and Payne.²¹⁾ The measurement was carried out at a frequency of 850 Hz with an amplitude of 5 mV, and at 7.0 s after the birth of a mercury drop whose total life was about 12 s in 1.0 M NaClO₄.

The capillaries used in the above two measurements were siliconed on the internal wall by passing a vapor of dimethyldichlorosilane for several seconds.

Polarographic measurement, in which an instantaneous current at the end of the drop life was recorded, were carried out with a three-electrode system consisting of a Yanagimoto Voltammetric Analyzer (Model P-1000). The drop time was adjusted to 3.5 s, and the flow rate of mercury was determined by weighing mercury recovered during a given time, and it was 1.781 mg s⁻¹ at a mercury height of 60 cm. The concentration of Eu(III) ion was 0.98 mM. Currents were corrected for the residual current which was measured independently. The true standard rate constant was obtained following the method due to Asada *et al.*²²⁾ The apparent heat of activation of the electrode reaction at the standard potential was determined from the dependence of the apparent standard rate constant on temperature.

All the measurements except for the apparent heat of activation were carried out in a water bath thermostated at 25 ± 0.1 °C, and potentials were measured against a saturated calomel electrode (SCE).

Results and Discussion

Electrocapillary and Differential Capacity-potential Curves.

[†] 1 M = 1 mol dm⁻³.

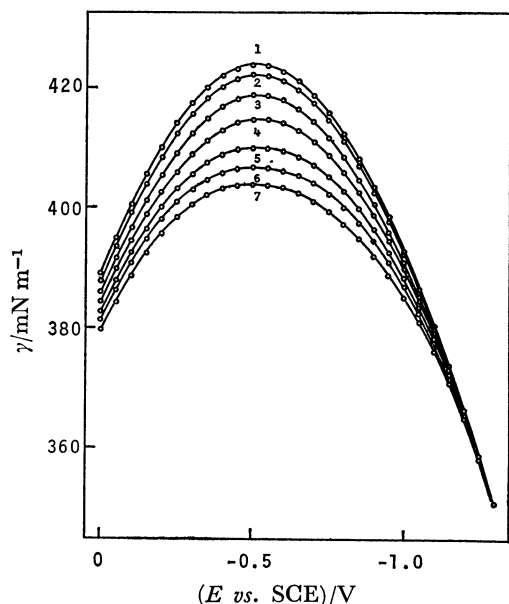


Fig. 1. Electrocapillary curves for aqueous 1.0 M NaClO_4 solutions containing 1,4-benzenedimethanol in various concentrations at 25 °C. The concentrations (mM): (1) 0 (base solution, 1.0 M NaClO_4), (2) 0.5, (3) 2.0, (4) 4.0, (5) 7.0, (6) 10.0, and (7) 15.0.

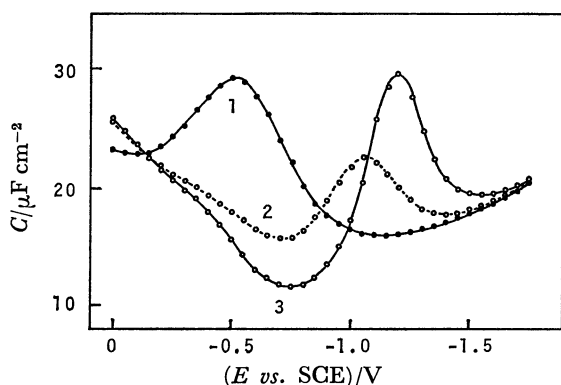


Fig. 2. Typical differential capacity-potential curves of the mercury electrode in aqueous 1.0 M NaClO_4 solutions with and without 1,4-benzenedimethanol at 25 °C. The concentrations of 1,4-benzenedimethanol (mM): 0 (base solution, 1.0 M NaClO_4), (2) 3.0, and (3) 15.0.

Figure 1 shows the electrocapillary curves obtained for the 1.0 M NaClO_4 containing 1,4-BDM in various concentrations. The drop in the interfacial tension, γ , due to an increase in the concentration is most remarkable at -0.5 V, which approximately corresponds to the electrocapillary maximum, E_{ecm} . This suggests that 1,4-BDM adsorbed on the electrode does not take an orientation with a large dipole moment in the direction normal to the electrode surface.

Figure 2 shows the typical differential capacity-potential curves obtained for the 1.0 M NaClO_4 containing 1,4-BDM. The adsorption-desorption peak at more positive potentials was not observed clearly, in contrast to that at more negative potential. This indicates that π -electrons in 1,4-BDM interact with the positive charge on the electrode, as have been

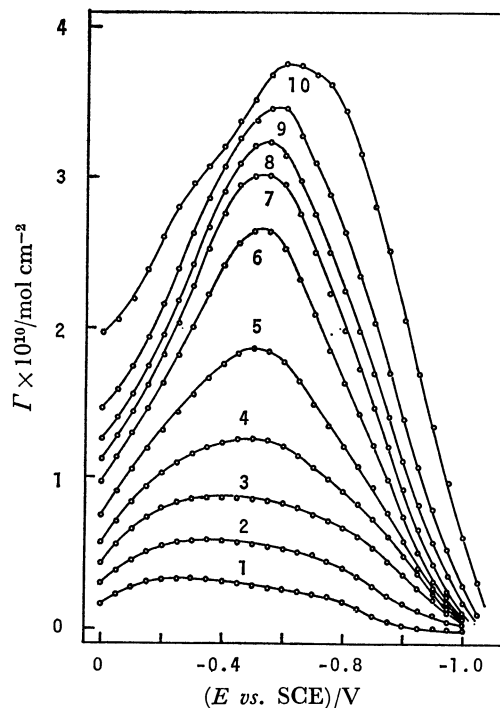


Fig. 3. Surface excess of 1,4-benzenedimethanol as a function of potential.

The concentrations of 1,4-benzenedimethanol (mM): (1) 0.2, (2) 0.5, (3) 1.0, (4) 1.4, (5) 2.0, (6) 3.0, (7) 4.0, (8) 5.0, (9) 7.0, and (10) 15.0.

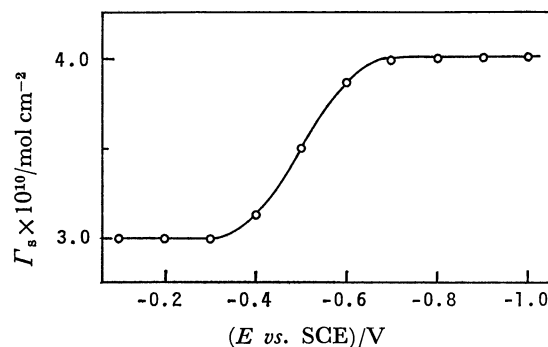


Fig. 4. Variation of surface excess at saturation, Γ_s , with the electrode potential.

accounted for in organic compounds with π -electrons.²³⁻²⁵⁾

The curve for the base 1.0 M NaClO_4 showed a large peak due to specific adsorption of perchlorate anion.²⁶⁾ However, the peak was diminished with an increase in the concentration of 1,4-BDM, and completely disappeared at more concentrated solutions than 1.0 mM. It was thought that the specific adsorption of perchlorate anion becomes unimportant at higher concentrations of 1,4-BDM.

Adsorption Behaviors. Surface excess, Γ , of 1,4-BDM was obtained using Eq. 1,

$$(\partial\gamma/\partial\ln C_{\text{org}})_{E,P,T} = -RT\Gamma, \quad (1)$$

where C_{org} is the concentration of 1,4-BDM, and the others have usual meaning. The surface excess at various concentrations is shown in Fig. 3 as a function of potential. Figure 4 shows a relation between the

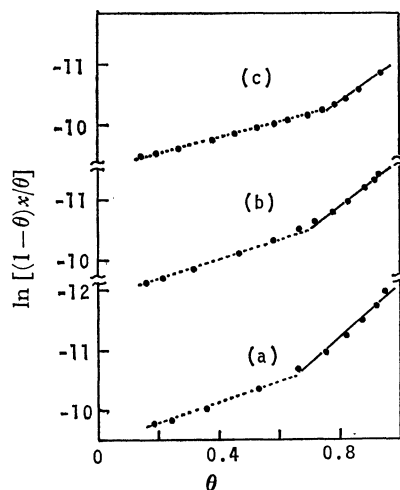


Fig. 5. Test of the Frumkin isotherm at different potentials. Potential and Γ_s used for the estimation of coverage: (a) -0.5 V and 3.5×10^{-10} mol cm $^{-2}$, (b) -0.6 V and 3.9×10^{-10} mol cm $^{-2}$, and (c) -0.7 V and 4.0×10^{-10} mol cm $^{-2}$.

potential and the surface excess at saturation, Γ_s , which are obtained by extrapolating the plots of $1/\Gamma$ vs. $1/C_{org}$ at a given potential to $1/C_{org}=0$. The value of Γ_s obtained in this way reflects the orientation at higher surface excess from the nature of the plots. Two limiting values of Γ_s were observed depending on the potential. One was 3.0×10^{-10} mol cm $^{-2}$ and the other was 4.0×10^{-10} mol cm $^{-2}$. Since the center of the change in Γ_s was -0.5 V which nearly corresponded to E_{ecm} , this change was thought to result from an interaction between π -electrons in the adsorbed 1,4-BDM molecules and the surface charge on the electrode. Then, it was considered that the lower value of Γ_s corresponds to a horizontal orientation and the higher one to a vertical orientation with a smaller projected area.

As the adsorption behavior of 1,4-BDM was expected to be complicated, it was somewhat closely examined by fitting to a Frumkin isotherm with two parameters, Γ_s and the interaction parameter. Equation 2 shows the Frumkin isotherm,

$$\beta x = \theta/(1-\theta) \exp(-2a\theta), \quad (2)$$

where β is the adsorption coefficient being a function of the standard free energy of adsorption, x and θ are the molar fraction and the coverage defined as Γ/Γ_s , respectively, and $2a$ is the interaction parameter whose positive (negative) value means that an attractive (repulsive) force acts among adsorbed molecules. The Frumkin isotherm plot at various potentials is shown in Fig. 5. The value of θ necessary for this plot was evaluated using the value of Γ_s corresponding to each potential in Fig. 4. In this treatment, it is assumed that the orientation of 1,4-BDM around E_{ecm} is intermediate between the horizontal and the vertical orientation, regardless of coverage. However, a linear relation over the whole coverage, which was actually observed for -0.2 and -0.9 V far from E_{ecm} , was not obtained for the potentials around E_{ecm} . A change in the orientation owing to coverage seems to be the cause, because the plots

TABLE 1. INTERACTION PARAMETER AT VARIOUS POTENTIALS

(Potential vs. SCE)/V	-0.4	-0.5	-0.6	-0.7	-0.8
$2a$	1.5	1.9	2.0	1.5	1.0

in Fig. 5 change the slope at higher coverage. It has already been described that aromatic compounds have a tendency to change the orientation with the surface charge on the electrode, namely a horizontal orientation at positive charge owing to attractive interaction with π -electrons and a vertical orientation at negative charge owing to repulsive interaction with π -electrons. Except for this electrostatic effect, at potentials around E_{ecm} where the surface charge density is low, the hydrophobic interaction between the adsorbate and the electrode with a structured water, and the need for an increased packing seem to control the orientation. From this point of view, 1,4-BDM around E_{ecm} was considered to take a horizontal orientation with higher hydrophobicity at lower surface excess and a vertical one with a smaller projected area at higher surface excess. Then, the Frumkin isotherm in Fig. 5 was replotted using $\Gamma_s=3.0 \times 10^{-10}$ mol cm $^{-2}$ for $\theta \leq 0.7$. In this case, the plot showed an inflection at $\theta \approx 0.8-0.9$. The values of $2a$ obtained from the above treatment are summarized in Table 1. They were positive, and it was found that the attractive interaction acts among the adsorbed 1,4-BDM molecules in the horizontal orientation. It was also observed that the interaction parameter changes with potential. Although the cause is not clear, a change in the configuration of the hydroxyl groups due to the electric field seems to be a cause.

There remains a problem how to interpret the intermediate values of Γ_s around E_{ecm} . It can be interpreted in connection with the consideration of the orientation state of 1,4-BDM at higher surface excess. Thus, 1,4-BDM begins to take the vertical orientation, as the coverage evaluated with respect to the horizontal orientation exceeds $0.8-0.9$. Then, the electrode surface is thought to be completely covered with 1,4-BDM molecules which consist of the two orientations. The fraction of the vertical orientation in the mixed two orientations increases with an increase in the surface excess, but the maximum fraction which is associated with the value of Γ_s changes with the potential or the surface charge on the electrode. Above consideration seems to be more natural than that of the intermediate orientation corresponding to each Γ_s , and was actually verified in the following discussion with respect to adsorption effect of 1,4-BDM on the electrode kinetics of Eu(III).

Orientation Model. Figure 6 shows the variation of E_{ecm} with the surface excess. E_{ecm} showed a slight cathodic shift with an increase in the surface excess, but at higher surface excess it showed a slight anodic shift oppositely. This result was thought to be another proof for the change in the orientation due to coverage. When 1,4-BDM is adsorbed without net dipole moment, one can expect a positive shift of E_{ecm} by 30 mV²⁷⁾ or 70 mV,²⁸⁾ which has been

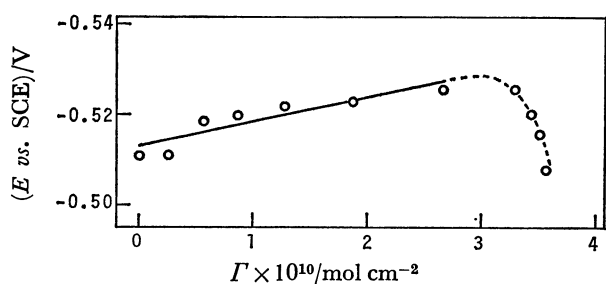


Fig. 6. Variation of the electrocapillary maximum, E_{ecm} , due to adsorption of 1,4-benzenedimethanol.

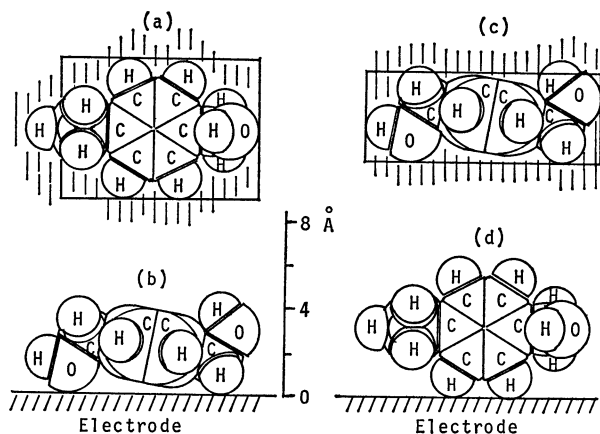


Fig. 7. Scale drawings of a 1,4-benzenedimethanol molecule adsorbed on the electrode through the horizontal orientation (a) and (b), and the vertical orientation (c) and (d). (a) and (c) show the top view, and (b) and (d) the side view. At the determination of the molecular configuration, the CPK precision molecular model was used.

estimated for the potential drop due to water dipoles at E_{ecm} . Therefore, the result in Fig. 6 can be interpreted as follows: the horizontal orientation at lower surface excess has a small dipole moment and at the interface the negative end of the dipole directs to the electrode, but the normal component of this dipole becomes unimportant with the change in the orientation from horizontal to vertical.

On the basis of the above consideration and the two different values of Γ_s , such orientation models as shown in Fig. 7 were considered for the horizontal and the vertical orientations at the potentials around E_{ecm} . The area of the rectangles enclosing the molecule in Figs. 7-a and 7-c are 55.3 \AA^2 or $3.0 \times 10^{-10} \text{ mol cm}^{-2}$ and 41.5 \AA^2 or $4.0 \times 10^{-10} \text{ mol cm}^{-2}$, respectively. Moreover, the height of the molecule estimated from Figs. 7-b and 7-d were about 4.2 \AA and 6.3 \AA , respectively. When these molecules form a monolayer on the electrode, the difference in the thickness of the layer can be expected to be about 2.1 \AA .

Kinetic Data for the Reduction of Eu(III) in the Presence of 1,4-BDM. In order to know the effect of π -electrons in 1,4-BDM on the reduction rate of Eu(III) ion, d.c. polarogram was measured with the aqueous 1.0 M NaClO_4 solution containing 0.98 mM Eu(III) ion and 1,4-BDM in various concentrations. Figure 8 shows the polarograms. It is obvious that

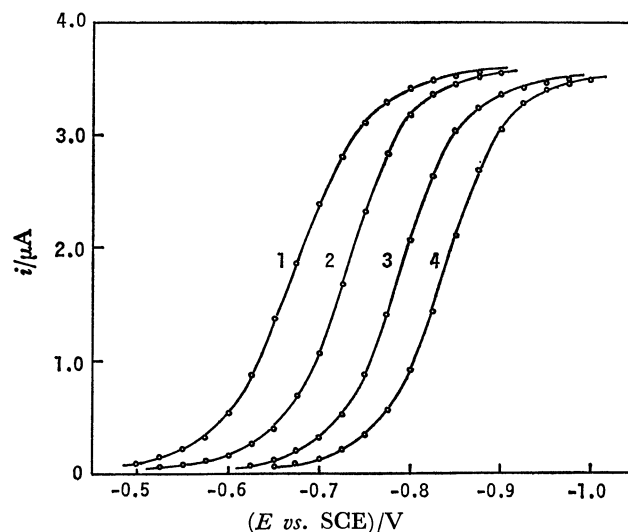


Fig. 8. D.c. polarograms of 0.98 mM Eu(III) ion in aqueous 1.0 M NaClO_4 solutions containing 1,4-benzenedimethanol at 25°C .

The concentrations of 1,4-benzenedimethanol (mM): (1) 0 (base solution, 1.0 M NaClO_4), (2) 1.0, (3) 4.0, and (4) 15.0.

the presence of 1,4-BDM in the solution inhibits the reduction of Eu(III) ion.

The true standard rate constant was determined from the analysis of the i - E curve at the foot of the wave ($i \leq 0.05 i_d$). Equation 3 represents the current for the reduction of Eu(III) to Eu(II),

$$i_0 = F A k_s^0 C_{\text{Eu(III)}}^0 \exp\{(\alpha - z) F \phi_2 / RT\} \exp(-\alpha F \eta / RT), \quad (3)$$

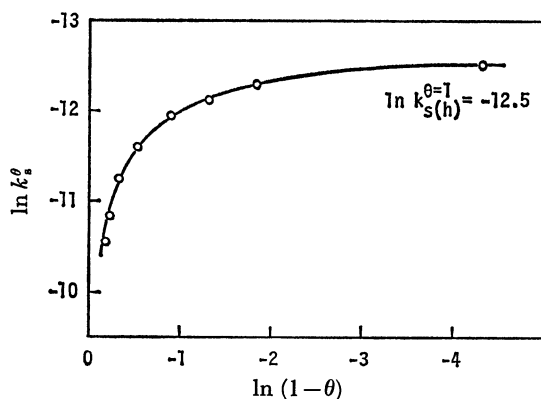
where A is the electrode area, $C_{\text{Eu(III)}}^0$ is the bulk concentration of Eu(III) ion, α is the true transfer coefficient, z is the ionic valence of Eu(III) ion, ϕ_2 is the inner potential at the outer Helmholtz plane which was determined using the Gouy-Chapman theory,²⁹⁾ η is the overpotential, k_s^0 is the true standard rate constant, and the others have usual meaning. As a first approximation, Eu(III) ion was assumed to take an electron at the outer Helmholtz plane with its hydration shell.³⁰⁾ Various kinetic data are summarized in Table 2 with the adsorption data of 1,4-BDM at the standard potential of Eu(III)/Eu(II) (-0.600 V vs. SCE ³¹⁾). For lower surface excess, the coverage θ was evaluated as Γ/Γ_s , where $\Gamma_s = 3.0 \times 10^{-10} \text{ mol cm}^{-2}$. However, for surface excess higher than $3.0 \times 10^{-10} \text{ mol cm}^{-2}$, the fraction of the vertical orientation in the mixture which consists of the vertical and the horizontal orientations, θ_v was estimated on the basis of the previous consideration of the full coverage. The diffusion constant of Eu(III), D , was constant throughout the solutions in an experimental error. On the other hand, the apparent heat of activation at the standard potential, ΔH_s^* , was increased with an increase in the coverage, but it came to constant near and at full coverage.

Inhibition Effect at Intermediate Coverage. The rate constant in the presence of organic adsorbates is generally a function of coverage, and it has been expressed in theoretical equations by considering various factors.

TABLE 2. ADSORPTION AND KINETIC DATA

Concn of 1,4-BDM mM	$\Gamma \times 10^{10}$ a) mol cm ⁻²	θ b)	θ_v c)	$E_{1/2}$ vs. SCE V	$k_s^\theta \times 10^6$ cm s ⁻¹	α	$D \times 10^6$ cm ² s ⁻¹	ΔH_s^* kJ mol ⁻¹
0 (base soln.)	—	—	—	-0.672	—	—	8.1	—
0.5	0.48	0.16	—	-0.709	25.8	0.39	8.2	—
0.7	0.62	0.21	—	-0.717	19.3	0.39	8.2	79.1
1.0	0.83	0.28	—	-0.734	13.0	0.40	8.1	—
1.4	1.22	0.41	—	-0.743	9.24	0.39	8.0	89.9
2.0	1.78	0.59	—	-0.757	6.61	0.36	8.2	—
2.5	2.20	0.73	—	-0.767	5.44	0.38	8.2	95.4
3.0	2.53	0.84	—	-0.773	4.59	0.40	8.3	—
4.0	2.96	0.99	—	-0.791	3.50	0.39	8.2	—
5.0	3.20	1.00	0.20	-0.799	2.65	0.44	8.2	94.1
7.0	3.50	1.00	0.50	-0.812	1.64	0.50	8.1	—
10.0	3.66	1.00	0.66	-0.824	1.15	0.56	8.2	—
15.0	3.79	1.00	0.79	-0.837	0.797	0.55	8.1	—
20.0	—	(1.00) d)	(0.90) d)	-0.848	0.773	0.59	8.1	95.8

a) The values at the standard potential of Eu(III)/Eu(II), -0.600 V vs. SCE. b) For the solutions up to 4 mM, the coverage θ was evaluated with the horizontal orientation, but in the solutions beyond 4 mM, the electrode surface was considered to be completely covered with a mixture consisting of the horizontal and the vertical orientations. c) The θ_v is the fraction of the vertical orientation in the mixture. d) Speculated values.

Fig. 9. Plot of $\ln k_s^\theta$ against $\ln(1-\theta)$.

The most simple form is the following equation,¹⁻³⁾

$$k_s^\theta = k_s^{\theta=0}(1-\theta) + k_s^{\theta=1}, \quad (4)$$

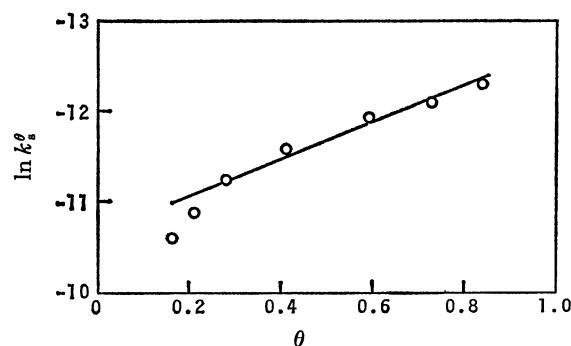
where $k_s^{\theta=0}$ and $k_s^{\theta=1}$ are the standard rate constants at zero and full coverage, respectively. Equation 4 is the sole equation that predicts a linear relation between k_s^θ and θ . When $k_s^{\theta=0} \gg k_s^{\theta=1}$, it changes to Eq. 5,

$$k_s^\theta = k_s^{\theta=0}(1-\theta), \quad (5)$$

which describes a simple blocking effect. However, Lipkowski and Galus³²⁾ have recently pointed out that the interpretation of Eq. 5 is different depending on the thermodynamics of the interface.

Figure 9 shows the plot of $\ln k_s^\theta$ against $\ln(1-\theta)$. In contrast to the prediction of Eq. 5, this plot showed a curvature. Further the plot based on Eq. 4 also showed a curvature, thus it was concluded that the electroreduction of Eu(III) ion in the presence of 1,4-BDM could not be described by Eqs. 4 and 5.

Afanas'ev and Ternovskoi⁸⁾ have presented the next equation which is one of the equations predicting

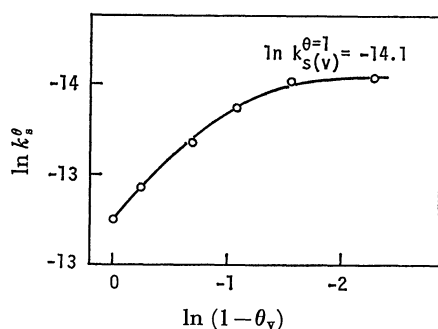
Fig. 10. Plot of $\ln k_s^\theta$ against θ .

a non-linear relation between k_s^θ and θ ,

$$k_s^\theta = k_s^{\theta=0} \exp(-2a\theta), \quad (6)$$

where $2a$ is the interaction parameter of the Frumkin isotherm for adsorbate in the absence of discharging ion, r is a coefficient taking into consideration the decrease in the attractive interaction between the adsorbed molecules when the discharging ion is transferred into the adsorbed layer. This equation is based on the consideration that the concentration of the discharging ion in the surface layer is determined by the additional energy ($2ar\theta RT$) required to transfer the discharging ions from the bulk of the solution into the structured surface layer consisting of water and the adsorbed molecules.

Figure 10 shows the plot based on Eq. 6 in the region of $\theta \leq 0.8$. A linear relation was observed in the region of $0.2 \leq \theta \leq 0.8$. The deviation of the plot from the linear relation in $\theta < 0.2$ seems to result from a specific adsorption of perchlorate anion which acts as an accelerator. The slope was 2.0 and it agreed well with the value of $2ar$ at $r=1$, 2.0 which was estimated from the fit to the Frumkin isotherm.

Fig. 11. Plot of $\ln k_s^0$ against $\ln(1-\theta_v)$.

It was pointed out in Ref. 8 that Eq. 6 is set up when the transfer of the discharging ion into the surface layer is reversible, while the electrode reaction rate is limited by the electron transfer step. Such a surface layer also does not influence the diffusion limiting current.³²⁾ The constancy of D in Table 2 satisfies the requirement. Further, the increase in ΔH_s^* due to adsorption of 1,4-BDM is thought to support the above inhibition effect, although the change is somewhat larger than that expected from the additional energy.

Inhibition Effect at Full Coverage. Figure 11 shows the plot of $\ln k_s^0$ against $\ln(1-\theta_v)$. The standard rate constant was diminished with an increase in θ_v , and showed a limiting value of -14.1 . A similar limiting value of -12.5 has also been observed in Fig. 9. Taking into consideration the adsorption behavior of 1,4-BDM, the former can be assigned to the rate constant relating to the vertical orientation $\ln k_{s(v)}^{\theta=1}$, indeed the vertical orientation at this time is not so perfect as in $E \leq -0.7$ V, and the latter to that relating to the horizontal one $\ln k_{s(h)}^{\theta=1}$. The difference between above two values was 1.6, and the inhibition effect due to the vertical orientation was larger than that due to the horizontal one.

It is also considerable for this result that the deformation of the structured surface layer is a factor for the inhibition of the electroreduction of Eu(III) ion at full coverage.

However, the process that Eu(III) ion penetrates into the adsorbed monolayer by surmounting only the deformation energy seems to be improbable at full coverage, because the penetration at full coverage needs another additional energy due to the displacement of 1,4-BDM adsorbed on the electrode, which is larger than the deformation energy and nearly the same as the adsorption energy, about 23 kJ mol^{-1} . As can be seen from Table 2, the values of ΔH_s^* near and at full coverage were approximately constant, regardless of the structure of the adsorbed monolayer. This result can not be explained by the penetration process based on the deformation or the displacement. As another factor for the inhibition effect at full coverage, the electron tunneling process through the adsorbed monolayer was considered. This process explains the constancy of ΔH_s^* . Thus, the reactant which accepts an electron at the tunneling transition is not Eu(III) ion at the ground state, but the ion at the activated state. Eu(III) ion is thought to be

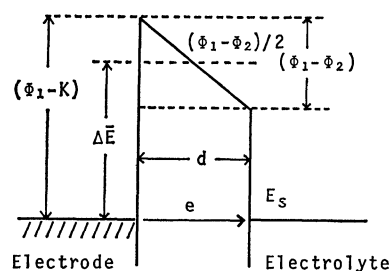


Fig. 12. Idealized rectangular barrier model for the electron tunneling from the mercury electrode to Eu(III) ion through the adsorbed 1,4-benzenedimethanol monolayer. Here, Φ_1 and Φ_2 are the electronic energy of the electrode and the electrolyte, respectively, K and $\Delta \bar{E}$ are the electron affinity of the monolayer and the mean height of the barrier, respectively, E_s is the standard potential of Eu(III)/Eu(II) in the absolute potential scale, and d is the thickness of the monolayer.

activated through the thermal and the electrostatic interactions of the ion with the surrounding water molecules, the so-called solvent rearrangement,³³⁾ and the energy necessary for such an activation can be expected to be independent of the surface layer structure, if a specific interaction between the reactant and the adsorbed molecules is not present.

Furthermore, appearance of the limiting value of $\ln k_s^0$ as shown in Fig. 9 has been attributed to a possibility of the electron tunneling through the adsorbed organic layer.³⁴⁾ Therefore, such a possibility was examined using the theory of elastic tunneling. Application of such a tunneling theory to the electrode kinetics has been carried out by Gurney³⁵⁾ and Gerisher,³⁶⁾ and has been verified by the experiment at the oxide covered electrodes.³⁷⁻⁴⁰⁾ The electron tunneling through organic monolayer between metals has also been verified with respect to various fatty acid salts.^{41,42)}

If the current at the electroreduction of Eu(III) ion is governed by the electron tunneling through the adsorbed organic monolayer, it is represented by Eq. 7,

$$i_{\theta=1} = e_0 \int_{-\infty}^{+\infty} \nu(E) N_b(E) D_{ox}(E) dE, \quad (7)$$

where e_0 is the charge of an electron, $N_b(E)$ and $D_{ox}(E)$ are the density of occupied electron states in the electrode and that of unoccupied states in the electrolyte, respectively, and $\nu(E)$ is the electronic frequency factor involving the tunneling probability. This tunneling probability is a function of the thickness of the adsorbed layer, d , and the mean height of the potential barrier, $\Delta \bar{E}$. On the basis of the idealized rectangular barrier model shown in Fig. 12, $\nu(E)$ is represented by the following equation,

$$\nu(E) \propto \exp\left\{-\left(4\pi d/h\right)\sqrt{2m_e\Delta\bar{E}}\right\}, \quad (8)$$

where h and m_e are Planck's constant and the mass of an electron, respectively. The frequency factor can be assumed to be independent of the energy, E . Further, assuming that $\Delta \bar{E}$ does not change with the

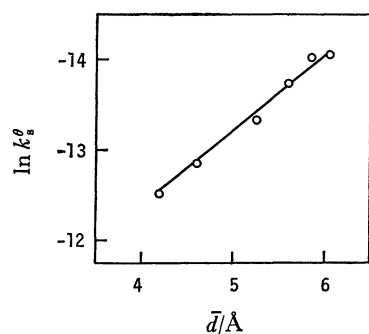


Fig. 13. Plot of $\ln k_s^0$ against \bar{d} .

orientation of 1,4-BDM, one obtains the next relation for the ratio of the true standard rate constant at full coverage with the horizontal and the vertical orientations,

$$\ln\{k_{s(v)}^0/k_{s(h)}^0\} = -(4\pi\Delta d/h)\sqrt{2m_e\Delta E}, \quad (9)$$

where Δd is the difference in the thickness of the adsorbed organic layer. The possibility of the electron tunneling process can be proved by using Eq. 9.

In general, $\Delta E = (\Phi_1 + \Phi_2)/2 - K$, where Φ_1 and Φ_2 are the electronic energy of the mercury used as the electrode and of the electrolyte, respectively, and K is the electron affinity of the adsorbed organic monolayer. One can use the work function of mercury and the standard potential of Eu(III)/Eu(II) in the absolute potential scale as Φ_1 and Φ_2 , respectively. One obtains 4.5 eV⁴³⁾ for Φ_1 , and 4.1 eV for Φ_2 using the value of 4.43 V⁴⁴⁾ as the absolute potential of the standard hydrogen electrode. Further, K is defined as $(I_p - E_g)$, where I_p and E_g are the ionization potential and the band gap of the adsorbed 1,4-BDM monolayer, respectively. These values must be actually for the monolayer, but those for the molecule were used. The value of E_g was evaluated from the ultraviolet spectrum measured in the 1.0 M NaClO₄ solution dissolved 1,4-BDM, and it was 5.69 eV for $\lambda_{\max} = 218$ nm. Since the value of I_p was not found in the literature, instead, that of benzenemethanol 9.14 eV⁴⁵⁾ was used.

Finally, one obtains 1.7 Å for Δd by introducing $\ln\{k_{s(v)}^0/k_{s(h)}^0\} = -1.6$ and the others into Eq. 9. Taking into consideration the imperfection of the adsorbed monolayer and rough approximations used, this calculated value of 1.7 Å seems to agree well with 1.9 Å, which was estimated by applying the arithmetic mean to Γ_s of 3.9×10^{-10} mol cm⁻² at -0.600 V on the basis of the consideration of the mixed orientation and the orientation model in Fig. 7.

Figure 13 shows the plot of $\ln k_s^0$ against the arithmetic mean thickness of the adsorbed layer saturated with the two orientations, \bar{d} . A linear relation observed in this Figure is considered to support the previous consideration of the full coverage at higher surface excess, and also the electron tunneling process through the adsorbed organic monolayer.

Concluding Remarks. In the results and the discussions so far mentioned, it was clarified that the

horizontal orientation of the benzene ring inhibited the electroreduction rate of Eu(III) ion, which is known as the reaction of simple charge transfer type. This result was distinct from that obtained by Loshkarev *et al.*¹³⁾ with respect to the reaction of deposition type. In considering that Eu(III) ion takes an electron with its hydration shell, the reduction intermediates of Bi(III) and Cd(II), which seem to be partially dehydrated, may have such an interaction with π -electrons that does not lead to the inhibition of charge transfer rate. However, the idea¹⁴⁾ that aromatic compounds adsorbed horizontally extend the electrode surface toward the solution side through the aromatic rings was not applicable to the system in this study.

References

- 1) J. Weber, J. Koutecký, and J. Koryta, *Z. Elektrochemie*, **63**, 583 (1959).
- 2) J. Kuta and I. Smoler, *Z. Elektrochemie*, **64**, 285 (1960).
- 3) W. Miller and W. Lorenz, *Z. Phys. Chem. (Frankfurt)*, **27**, 23 (1961).
- 4) K. K. Niki and N. Hackerman, *J. Electroanal. Chem.*, **32**, 257 (1971).
- 5) F. Scheller, R. Landsberg, and H. Wolf, *Z. Phys. Chem. (Leipzig)*, **244**, 273 (1970).
- 6) J. Lipkowski and Z. Galus, *J. Electroanal. Chem.*, **39**, 333 (1972).
- 7) R. Parsons, *J. Electroanal. Chem.*, **21**, 35 (1969).
- 8) B. N. Afanas'ev and L. A. Ternovskoi, *Elektrokhimiya*, **10**, 901 (1974).
- 9) R. Parsons, *Adv. Electrochem. Electrochem. Eng.*, **1**, 1 (1961).
- 10) S. Sathyanarayana, *J. Electroanal. Chem.*, **50**, 195 (1974).
- 11) J. Lipkowski and Z. Galus, *J. Electroanal. Chem.*, **61**, 11 (1975).
- 12) B. B. Damaskin and B. N. Afanas'ev, *Elektrokhimiya*, **13**, 1099 (1977).
- 13) Yu. M. Loshkarev, V. V. Trofinenko, and A. A. Kuznetsov, *Elektrokhimiya*, **11**, 1724 (1975).
- 14) S. L. Dyatkina and B. B. Damaskin, *Elektrokhimiya*, **2**, 1340 (1966).
- 15) E. Dutkiewicz and A. Paucz, *J. Electroanal. Chem.*, **100**, 947 (1979).
- 16) D. J. Schiffrin, *J. Electroanal. Chem.*, **23**, 168 (1969).
- 17) O. Ikeda, Y. Matsuda, H. Yoneyama, and H. Tamura, *Electrochim. Acta*, **21**, 519 (1976).
- 18) A. De Battisti and S. Trasatti, *J. Electroanal. Chem.*, **54**, 1 (1974).
- 19) D. M. Mohilner and H. Nakadomari, *J. Phys. Chem.*, **77**, 1594 (1973).
- 20) D. M. Mohilner, L. W. Browman, S. J. Freeland, and H. Nakadomari, *J. Electrochem. Soc.*, **120**, 1658 (1973).
- 21) G. J. Hills and R. Payne, *Trans. Faraday Soc.*, **61**, 316 (1965).
- 22) K. Asada, P. Delahay, and A. K. Sundaram, *J. Am. Chem. Soc.*, **83**, 3396 (1961).
- 23) M. A. Gerovich and G. F. Rybalchenko, *Zh. Fiz. Khim.*, **32**, 109 (1958).
- 24) E. Blomgren and J. O'M. Bockris, *J. Phys. Chem.*, **63**, 1475 (1959).
- 25) B. E. Conway and R. G. Barradas, *Electrochim. Acta*, **5**, 319 (1961).
- 26) R. Payne, *J. Phys. Chem.*, **70**, 204 (1966).
- 27) J. O'M. Bockris and M. A. Habib, *Electrochim. Acta*,

- 22, 41 (1977).
28) S. Trasatti, *J. Electroanal. Chem.*, **91**, 293 (1978).
29) D. C. Grahame, *Chem. Rev.*, **41**, 441 (1947).
30) C. W. De. Kreuk, M. Sluyters-Rehbach, and J. H. Sluyters, *J. Electroanal. Chem.*, **28**, 391 (1970).
31) L. Gierst and P. Cornelissen, *Collect. Czech. Chem. Commun.*, **25**, 3004 (1960).
32) J. Lipkowski and Z. Galus, *J. Electroanal. Chem.*, **98**, 91 (1979).
33) D. B. Matthews and J. O'M. Bockris, "Modern Aspects of Electrochemistry," ed by J. O'M. Bockris and B. E. Conway, Butterworth, London (1971), Vol. 6, p. 242.
34) J. Lipkowski, E. Kosińska, M. Goledzinowski, J. Nieniewska, and Z. Galus, *J. Electroanal. Chem.*, **59**, 344 (1975).
35) R. W. Gurney, *Proc. R. Soc. London, Ser. A*, **134**, 137 (1932).
36) H. Gerisher, *Z. Phys. Chem. N. F.*, **26**, 223, 325 (1960).
37) J. W. Schultze and K. J. Vetter, *Electrochim. Acta*, **18**, 889 (1973).
38) J. W. Schultze and U. Stimming, *Z. Phys. Chem. N.F.*, **98**, 285 (1975).
39) K. E. Heusler and M. Schultze, *Electrochim. Acta*, **20**, 237 (1975).
40) W. Schmickler and J. Ulstrup, *Chem. Phys.*, **19**, 217 (1977).
41) B. Mann and H. Kuhn, *J. Appl. Phys.*, **42**, 4398 (1971).
42) E. E. Polymeropoulos, *J. Appl. Phys.*, **48**, 2404 (1977).
43) S. Trasatti, *Adv. Electrochem. Electrochem. Eng.*, **10**, 213 (1977).
44) A. Henglein, *Ber. Bunsenges. Phys. Chem.*, **78**, 1078 (1974).
45) S. Pignataro, A. Foffani, G. Innorta, and G. Distefano, *Z. Phys. Chem. N.F.*, **49**, 291 (1966).
-